ACS MEASUREMENT SCIENCE Au
AN OPEN ACCESS JOURNAL OF THE AMERICAN CHEMICAL SOCIETY

pubs.acs.org/measureau
Article

Rapid and Robust Workflows Using Different Ionization, Computation, and Visualization Approaches for Spatial Metabolome Profiling of Microbial Natural Products in *Pseudoalteromonas*

Jian Yu, Haidy Metwally, Jennifer Kolwich, Hailey Tomm, Martin Kaufmann, Rachel Klotz, Chang Liu, J. C. Yves Le Blanc, Thomas R. Covey, John Rudan, Avena C. Ross, and Richard D. Oleschuk*

Cite This: *ACS Meas. Sci. Au* 2024, 4, 668–677
Read Online

ABSTRACT: Ambient mass spectrometry (MS) technologies have been applied to spatial metabolomic profiling of various samples in an attempt to both increase analysis speed and reduce the length of sample preparation. Recent studies, however, have focused on improving the spatial resolution of ambient approaches. Finer resolution requires greater analysis times and commensurate computing power for more sophisticated data analysis algorithms and larger data sets. Higher resolution provides a more detailed molecular picture of the sample; however, for some applications, this is not required. A liquid microjunction surface sampling probe (LMJ-SSP) based MS platform combined with unsupervised multivariant analysis based hyperspectral visualization is demonstrated for the metabolomic analysis of marine bacteria from the genus *Pseudoalteromonas* to create a rapid and robust spatial profiling workflow for microbial natural product screening. In our study, metabolomic profiles of different *Pseudoalteromonas* species are quickly acquired without any sample preparation and distinguished by unsupervised multivariant analysis. Our robust platform is capable of automated direct sampling of microbes cultured on agar without clogging. Hyperspectral visualization-based rapid spatial profiling provides adequate spatial metabolite information on microbial samples through red–green–blue (RGB) color annotation. Both static and temporal metabolome differences can be visualized by straightforward color differences and differentiating m/z values identified afterward. Through this approach, novel analogues and their potential biosynthetic pathways are discovered by applying results from the spatial navigation to chromatography-based metabolome annotation. In this current research, LMJ-SSP is shown to be a robust and rapid spatial profiling method. Unsupervised multivariant analysis based hyperspectral visualization is proven straightforward for facile/rapid data interpretation. The combination of direct analysis and innovative data visualization forms a powerful tool to aid the identification/interpretation of interesting compounds from conventional metabolomics analysis.

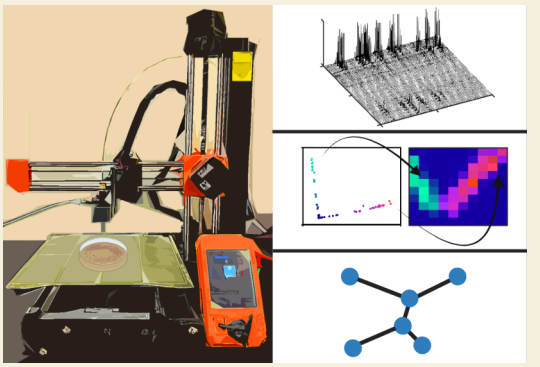

KEYWORDS: *mass spectrometry, rapid analysis, spatial metabolome, natural products, ambient ionization*

INTRODUCTION

Mass spectrometry (MS) has been extensively used in metabolome research as a powerful tool in molecular characterization for various compounds.[1] Compared with other compound characterization techniques such as nuclear magnetic resonance (NMR), the superior sensitivity and selectivity of MS make it a robust tool for higher-throughput metabolome analysis.[2] However, labor-intensive sample preparation steps such as filtration and/or solvent extraction are still necessary for MS detection of biomarkers or natural product discovery.[2,3]

Ambient ionization MS was invented to minimize sample preparation and, in some cases, enable researchers to test samples directly.[4] Since the first reports of ambient ionization, significant progress has been made to improve the spatial resolution for metabolomic analysis.[5−10] With the development of precise sampling techniques, the state-of-the-art resolution for spatial metabolome research has reached ∼10 μm levels.[8,11,12] Although impressive applications such as single cell analysis[13] or early tumor diagnosis[14] have been achieved in the past decade, micrometer-level spatial resolution introduces issues such as extended sampling time, complicated equipment alignment, and exhaustive troubleshooting.[15,16] No doubt high spatial resolution can be critical for some applications; however, robustness and throughput can be

Received: July 2, 2024
Revised: August 30, 2024
Accepted: September 3, 2024
Published: October 21, 2024

https://doi.org/10.1021/acsmeasuresciau.4c00035
ACS Meas. Sci. Au 2024, 4, 668–677

more important for research applications such as colony level microbial analysis.[17]

In our previous studies, the liquid microjunction surface sampling probe (LMJ-SSP) and MS combined with hyperspectral visualization were effective for the *in situ* analysis of bacterial colonies.[18,19] To compare the performance of the LMJ-SSP with other profiling techniques and further demonstrate hyperspectral based data visualization in different scenarios, a rapid and robust workflow for spatial metabolomics was explored in the current study. Gram-negative marine bacteria from the genus *Pseudoalteromonas*, which has become popular for its production of highly conjugated natural products with unique structures and interesting bioactivities, was chosen for workflow demonstration.[20]

In our current study, the LMJ-SSP is shown to generate robust data for the *in situ* analysis of a single microbial colony and to be compared to other mainstream ambient ionization techniques. One millimeter spatial resolution of the LMJ-SSP is shown to be adequate for the preliminary screening of natural products. Hyperspectral visualization workflow, which converts static or temporal metabolomic features into red−green−blue (RGB) coded colors, is tested with distinct MS data visualization techniques and different types of multivariant analysis algorithms. Results from spatial metabolome analysis are further used to navigate the data analysis for a liquid chromatography−mass spectrometry (LC−MS) based metabolomics experiment. Analogues of Tambjamine YP1,[21] which possess fatty acid amine tails of different lengths, are quickly identified from a large molecular network of *Pseudoalteromonas tunicata* with the aid of spatial profiling. LMJ-SSP and hyperspectral visualization based spatial profiling workflow are demonstrated as an efficient method to assist microbial metabolome analysis.

EXPERIMENTAL SECTION

Materials

HPLC-grade methanol, formic acid, and α-cyano-4-hydroxycinnamic acid (HCCA) were sourced from Sigma-Aldrich (Saint Louis, US). Deionized water was obtained with a Sartorius Arium Pro DI Ultrapure Water System (Gottingen, Germany). Microscope glass slides were purchased from Fisher Scientific (Hampton, US). Indium tin oxide (ITO) coated slides were purchased from Bruker (Billerica, US).

Bacteria Sample Preparation

Agar plates with bacterial colonies were prepared using a modified drop plate method.[22] As described in previous research,[18] *Pseudoalteromonas rubra* DSM6842, *Pseudoalteromonas tunicata* DSM14096, *Pseudoalteromonas piscicida* JCM20779, and *Pseudoalteromonas elyakovii* ATCC700519 are streaked on Difco Marine Broth 2216 (Mar2216) agar (1%) and incubated overnight at 30 °C. Each species of *Pseudoalteromonas* is picked as a single colony from their respective plate, inoculated into liquid Mar2216 broth (5 mL), and incubated overnight at 30 °C with shaking at 170 rpm. The overnight cultures are diluted 10-fold and dropped in ∼20 μL aliquots onto a fresh Mar2216 agar (1%) plate that is divided into four quadrants. The distance between strains or colonies is not strictly controlled. The plate is incubated at 30 °C for about 5 days and stored at 4 °C awaiting analysis.

Agar plates used for microbial interaction analysis are prepared with a modified cross streak method.[23,24] *Pseudoalteromonas rubra* DSM6842 and *Pseudoalteromonas tunicata* DSM14096 are cross-strewn in the shapes of "+" and "V" to examine their interaction zones. Plates for static analysis are incubated at 30 °C overnight and stored at 4 °C awaiting analysis. Plates for temporal experiments are tested 1 h after incubation and 24 h afterward.

Direct Sampling by LMJ-SSP

The liquid microjunction surface sampling probe (LMJ-SSP), which was originally designed by Van Berkel,[25,26] was used for the direct analysis of microbial colonies. As described in Figure S1, the sampling probe is composed of two concentric tubes (outer tube: 762 μm I.D. × 1588 μm O.D., length ∼5 cm; inner tube: 250 μm I.D. × 350 μm O.D., length ∼25 cm) and a metal "tee" union.[18] Methanol, which is delivered by an HPLC pump at 200 μL/min, was chosen as a carrier liquid for performance based upon previous studies.[18,27]

To evaluate the performance of LMJ-SSP, an agar plate inoculated with *P. rubra* (shown in Figure 1A and Figure S2) was sampled directly by LMJ-SSP. The MS (SCIEX 4500 triple quadrupole, Concord, ON, Canada), which was connected to an LMJ-SSP, was operated with full scan function (m/z 300−400, 2000 Da/s) in positive ion mode (spray voltage = +5500 V, curtain gas = 20 arbitrary units, gas 1 = 80 arbitrary units, gas 2 = 30 arbitrary units).

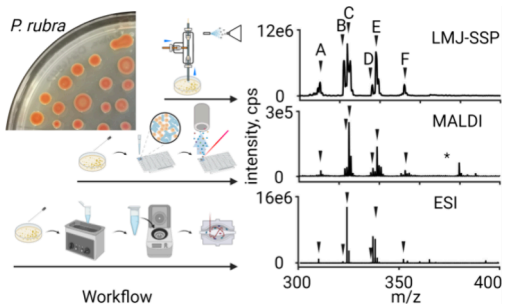

Figure 1. Example of typical workflows and spectra of *P. Rubra* using different rapid mass spectrometry detection methods (LMJ-SSP, MALDI and Direct Infusion) (A: $C_{19}H_{23}N_3O$, 2-methyl-3-butyl prodigiosin, m/z 310.2; B: $C_{20}H_{23}N_3O$, cycloprodigiosin, m/z 322.2; C: $C_{20}H_{25}N_3O$ prodigiosin, m/z 324.2; D: $C_{21}H_{25}N_3O$, predicted prodiginine, m/z 336.2; E: $C_{21}H_{27}N_3O$, 2-methyl-3-hexyl prodigiosin, m/z 338.2, F: $C_{22}H_{29}N_3O$, 2-methl-3-heptyl prodigiosin m/z 352.2, *: signal from α-cyano-4-hydroxycinnamic acid).

Direct Analysis by MALDI

MALDI time-of-flight (TOF) mass spectrometry was chosen as the reference method because it has been widely used in various microbial analyses.[28,29] Similar to the protocol of the popular Biotyper,[30] a syringe needle was used to scrape a tiny piece of colony (*P. rubra* DSM6842) onto the MALDI target plate. Two microliters of HCCA solution (7 mg/mL, ACN/H_2O = 1/1) was dripped onto the sample and left until the sample is completely dry. A full scan (m/z 200−5000, positive mode) was used to test the sample (Bruker Autoflex Speed MALDI TOF, Bremen, Germany)

Direct Infusion-Based MS Analysis

A straightforward extraction-based protocol combined with electrospray ionization, high-resolution mass spectrometry, and direct infusion was used as another reference. Several colonies of *P. rubra* were transferred into a 15 mL polypropylene centrifuge tube (Corning Inc., Corning, USA) with 10 mL of methanol/H_2O = 1/1. The tube was vortexed and sonicated for 30 min. The sample was centrifuged at 10,000*g* for 5 min to remove particles prior to direct infusion-based high-resolution mass spectrometry analysis. A gastight syringe (500 μL, Hamilton Co., Reno, USA) was used to infuse the sample into an LTQ Orbitrap Velos Pro (ThermoFisher, San Jose, CA, USA) directly for analysis. An ESI source (positive mode, spray voltage = 3500 V, sheath gas flow rate = 10 arb, aux gas flow rate = 0 arb, capillary temperature = 290 °C) and full scan (m/z 300−400) were used for the analysis. The Xcalibur 2.2 SP1 software was used to control the instrument.

https://doi.org/10.1021/acsmeasuresciau.4c00035
ACS Meas. Sci. Au 2024, 4, 668−677

Conductance-Based Autosampling by LMJ-SSP

A conductance feedback loop based 3D printer platform,[19] which moves the probe in a "stepping sampling mode",[26] was developed by our lab to facilitate autoimaging of uneven microbial colonies.[19] During the automated imaging process, the probe touches the sample surface for 2 s and travels for 30 s to the next pixel.[18] Unlike other popular mass spectrometry imaging (MSI) techniques, no sample preparation or extensive alignment is needed for the imaging, and samples remain intact after imaging.[18,19] Simply pointing the probe to the starting point for imaging and positioning it several centimeters above the sample is enough to begin the imaging experiment.

To evaluate the performance of LMJ-SSP in various microbial analyses, MSI experiments were conducted directly upon agar plates. Areas with a single colony of *P. tunicata* (Figure S2B2, 8 × 10 mm) were sampled to demonstrate the robustness of the LMJ-SSP based autosampling platform. Cross streaked *P. rubra* and *P. tunicata* (Figure S2C,D, 10 × 15 mm) were directly sampled to demonstrate how microbial interaction analysis can be facilely performed. To demonstrate the potential of using LMJ-SSP in temporal microbial monitoring, cross streaked *P. rubra* and *P. tunicata* (Figure S2E, 10 × 10 mm) were sampled at 1 and 24 h after inoculation. Spatial resolution of imaging experiments in the current research was set at ≈1 mm. Further details of the sampling platform and sampling protocol can be found in a previous publication.[18,19]

MALDI-Based MSI

MALDI is the most popular MSI technique. To evaluate the LMJ-SSP based MSI protocol, MALDI was used as a "commercialized reference method". Unlike DESI or the LMJ-SSP, matrix deposition and sample preparation are necessary for MALDI. HCCA was chosen as a universal matrix for the positive mode MALDI. A homogeneous matrix deposition method[31,32] was modified for the agar plate. The targeted area was first cut from the plate and placed on a conductive ITO slide for dehydration. Air bubbles were avoided to ensure adequate adhesion. The excised agar was heated at 40 °C for ≈60 min in a fume hood to partially dehydrate the sample. Then a lab-developed matrix spray chamber was used for matrix deposition (spray time: 10 s, settle time: 10 s, drying time: 15 s, for 60 cycles). Note that it is important that some moisture remains in the agar after the first drying step to facilitate the crystallization of the matrix. After deposition, the agar was again dehydrated in a desiccator for 60 min. After the sample preparation procedure is completed, the agar should appear as depicted in Figure S3. The sampled area was then scanned by a Bruker Autoflex speed MALDI TOF in positive mode (m/z 150−2000, spatial resolution: 150 μm).

DESI-Based MSI

DESI, a commonly employed MSI technique,[33,34] was chosen as an additional reference MSI technique to evaluate the performance of the LMJ-SSP based MSI protocol. Usually, no sample preparation is needed if samples have a solid and flat surface.[35,36] But for our sample (Figure S2B2), the gel-like colony is very fragile to the gas flow emanating from the probe. Therefore, a dehydration protocol[37] is needed to ensure that the surface will be solid and flat after processing. A piece of agar slightly larger than the target colony was cut from the plate. The excised piece (size ∼2 × 2 cm) was placed on a glass slide that was then fixed to the heated bed of the 3D printer. Air bubbles were removed to ensure that the agar adhered well to the glass slide. The slide was maintained at 40 °C for ≈2 h in the fume hood. For most agar plate based imaging, only specially prepared thin layer agar plates are used for facile dehydration.[37] Extremely thin agar plates, however, limit the growth of colonies. The current protocol is designed for and compatible with agar plates with different thicknesses. It is important to visually confirm that the agar is getting thinner but not flaky (Figure S2B1) and that the agar still adheres well when heating is completed. Subsequently, it is important to keep the slide in a sealed box or tubing to prevent overdehydration. The imaging was conducted using a Waters Q-TOF instrument (Xevo G2-XS quadrupole time-of-flight QTOF, Waters, United States) equipped with a DESI source (DESI XS, Waters, United States). A full scan (m/z 50−1200, increment = 0.02, MS resolution = 20000) in positive mode was used to scan an area of 25.5 mm^2 (Figure S2B1, sampled area ∼15 × 1.7 mm). The spatial resolution was set to 100 μm.

Hyperspectral Visualization Based Spatial Metabolome Profiling

Hyperspectral visualization, which converts highly dimensional data into straightforward color codes through unsupervised multivariant analysis, has proven effective in the spatial profiling of microbial samples.[18,38] Multivariant analysis was first performed on the MS data set to decrease the dimensionality of the data set. A scoring plot was produced to visualize the clustering status of the data set. The score for each sampling spot/pixel in the first three dimensions was translated into red, green, and blue (RGB) values. By assigning RGB values to the corresponding sampling spot/pixel, a colorful map of the sampled area was constructed. The features of the MS data set, which are different m/z values/ranges, were plotted in the form of a heatmap.[18] All hyperspectral visualization related data analyses were performed by using MATLAB. A relative mass range was plotted in the heatmaps to reflect the complexity of the matrix on spectral acquisition and maintain isotopic information to help confirm molecular signals.

To demonstrate the robustness of the hyperspectral visualization workflow, data sets from different ionization techniques (DESI and LMJ-SSP) were tested under two typical types of multivariant analysis algorithms (PCA: principal component analysis and t-SNE: t-distributed stochastic neighbor embedding).[38] The analysis of *P. tunicata* by DESI (Figure S2B1) was tested to demonstrate that the hyperspectral visualization is not limited to data obtained using the LMJ-SSP only. Both PCA (typical linear algorithm) and t-SNE (typical nonlinear algorithm) were tested in the analysis of *P. rubra* and *P. tunicata* (Figure S2B1,D) to show that the workflow is not algorithm specific.[38,39] To further explore an innovative unsupervised data analysis method for temporal MSI research, hyperspectral visualization was used on cross streaked *P. rubra* and *P. tunicata* (Figure S2E) at 1 and 24 h after inoculation. Straightforward color differences, instead of complicated MS spectra, were used to visualize the metabolomic features of the sample.[18]

LC−MS Based Metabolomics Analysis

Conventional LC−MS based metabolomics analysis of *P. tunicata* extracts was performed. In a similar manner to the extraction protocol for *P. rubra* mentioned above, several colonies of *P. tunicata* were extracted in a 15 mL polypropylene centrifuge tube (Corning Inc., Corning, USA) with 10 mL of methanol/H_2O = 1/1. A combination of vortexing and 30 min of sonication was used to facilitate extraction. The supernatant was transferred into a 2 mL HPLC vial after centrifuging (at 10,000g, 5 min). An Agilent 1260 liquid chromatograph (Agilent Technologies, Santa Clara, CA, USA) combined with high-resolution MS (LTQ Orbitrap Velos Pro, ThermoFisher, San Jose, CA, USA) was used for metabolomics analysis of the extract of *P. tunicata*. A reversed phase C18 column (2.1 × 50 mm, 1.7 μm, Agilent Technologies, Santa Clara, CA, USA) was used for chromatographic separation. The mobile phase consisted of methanol (solvent A) and 0.1% formic acid (solvent B). The gradient was as follows: 15% solvent A from 0 to 3 min, 15−65% solvent A from 3 to 28 min, 65−95% solvent A from 28 to 30 min, 95% solvent A from 30 to 40 min, 95−15% solvent A from 40 to 41 min, and 15% solvent A from 41 to 50 min. The flow rate was 0.3 mL/min, and the injection volume was 1 μL. The ESI source condition was set as follows: positive mode, heater temperature = 350 °C, sheath gas flow rate = 30 arb, aux gas flow rate = 10 arb, spray voltage = 3.5 kV, and capillary temperature = 290 °C. The MS scanning method was set as follows: MS1 full scan: m/z 150−2000, MS1 resolution: 30000, data dependent MS2 = top 10, collision type = collision induced dissociation (CID), fragmentation energy = 30 V (normalized). Raw data were uploaded to GNPS (Global Natural Products Social Molecular Networking) for metabolite annotation (molecular networking workflow).[40]

https://doi.org/10.1021/acsmeasuresciau.4c00035
ACS Meas. Sci. Au 2024, 4, 668−677

RESULTS AND DISCUSSION

LMJ-SSP Based Direct Sampling Workflow vs Conventional Direct Sampling Workflow

To evaluate the performance of various direct sampling methods of MS, *P. rubra* is chosen as an example as it is already known to produce various prodiginine compounds.[20] As described in the Experimental Section, results from LMJ-SSP based direct sampling, MALDI-TOF, and direct infusion-based ESI-MS analysis are presented in Figure 1. Known prodiginine compounds[20] (A: $C_{19}H_{23}N_3O$, 2-methyl-3-butyl prodigiosin, m/z 310.2; B: $C_{20}H_{23}N_3O$, cycloprodigiosin, m/z 322.2; C: $C_{20}H_{25}N_3O$, prodigiosin, m/z 324.2; D: $C_{21}H_{25}N_3O$, predicted prodiginine, m/z 336.2[41]; E: $C_{21}H_{27}N_3O$, 2-methyl-3-hexyl prodigiosin, m/z 338.2, F: $C_{22}H_{29}N_3O$, 2-methl-3-heptyl prodigiosin m/z 352.2) can be easily spotted from spectra generated from all three methods. Although the MS resolution from the LMJ-SSP is much lower than that of the other analyzer because of the low resolution of tandem quadrupole MS, it does not limit the identification of the prodiginine compounds. Furthermore, there is only a small difference in sensitivity observed among the three spectra from Figure 1. This is to say, for the preliminary screening of microbial samples for dominating metabolites, the quality of data obtained from our LMJ-SSP/MS based workflow is sufficient.

Although methods such as MALDI and direct infusion ESI can both generate spectra with similar quality, they each have different requirements for sample preparation. For direct infusion-based MS analysis, particles that can clog the tubing and the use of a matrix that can suppress the ionization are some of the most significant problems preventing researchers from direct sampling. A classic liquid extraction process is therefore usually required. Such a process would usually require at least half an hour of sample preparation procedures, such as sonication, centrifugation, or filtration. Finally, several colonies are usually needed to increase the concentration of the extract. For MALDI, although protocols like that used by Biotyper[30] can be finished within minutes, significant time is still needed to transfer the microbial colony sample from the agar plate to the target plate and deposit the matrix solution for cocrystallization. Researchers also need to purchase and regularly prepare costly matrix solutions for MALDI. For analysis with the LMJ-SSP, no sample preparation is required, and raw microbial colonies remain intact after sampling as the LMJ-SSP uses a liquid bridge between probe tip and sample to acquire analyte/signal.[27] The cost for cleaning or replacement of the tee-joint and fused silica tubing is also very low.

We have developed a rapid and robust workflow for direct MS analysis on microbial samples using the LMJ-SSP In this application, the data provided by the LMJ-SSP (with no sample preparation) are similar to those generated by both DESI and MALDI approaches. However, alternative ionization approaches may be well suited to different analyte classes (e.g., proteins), which may impact method suitability. To further increase the throughput for data analysis, a lab developed software approach is also under development to automate the discovery of potential natural products from large data sets.

LMJ-SSP vs MALDI and DESI in Microbial Spatial Metabolome Profiling

MALDI is a classic technique for spatial metabolome research. The high spatial resolution of MALDI has been demonstrated in various fields, but sample preparation requirements[31,42,43] are potential challenges to its further application. MALDI sample preparation for colonies of *P. rubra* and *P. tunicata* includes dehydration and matrix deposition. Dehydration processes for agar need to be monitored continuously to ensure that the dehydrated agar piece remains flat and adheres well to the ITO slide. It is difficult to use many parameters from literature references directly because the majority use an extremely thin (≈1 mm) agar sample designed for a short-term incubation that is not compatible with natural product time frames.[44,45] It is critical to ensure that sample surfaces are flat during and after the matrix deposition and crystallization steps. Overdehydration makes the sample surface flaky and unable to absorb matrix solution. Adhesion is essential to make sure that the sample does not detach when exposed to the vacuum. Continuous visual inspection of matrix deposition is critical to ensure that a homogeneous matrix layer is established on the agar sample.[31] It is important that analytes and matrix are cocrystallized through recurring spray cycles and dehydration in a desiccator.[31] This entire process requires significant expertise and experience and is time-consuming.

DESI[46] has been widely used in spatial metabolomics for its simplified sample preparation process. Despite its extensive application, DESI is sensitive to the texture of the sample surface.[35] Both solid and flat surfaces are needed for DESI to maintain the consistency of signal and spatial resolution due to the desorption momentum-transfer-based mechanism.[36,37,47] For sampling of microbial colonies, a dehydration process that requires significant manual dexterity and practice (≈2 h of processing time) is therefore required to ensure the performance of DESI.

Alternatively, our LMJ-SSP based workflow is more time efficient with regard to sample preparation and data acquisition. The liquid bridge on the probe tip, which minimizes the contact between the sample and probe, makes direct microbial colony sampling possible.[26,27] Significant time normally required for spatial alignment is saved because the surface topology of the raw sample can be ignored when using a conductance feedback loop sampling platform.[19] Sample preparation for MALDI or DESI would cost hours in dehydration or matrix deposition, whereas a raw microbial colony can be directly assessed using the LMJ-SSP. Because of the coarser spatial resolution for the LMJ-SSP (1 mm), fewer pixels are needed to finish sampling. Therefore, the spatial profiling of an entire colony (≈1 cm diameter) can be completed in ≈1 h, whereas imaging only a portion of the colony (Figure 2C) took close to 2 h using DESI. A consideration for direct sampling is that the sample is still growing/dynamic (unlike MALDI/DESI where growth is halted during sample preparation); if there were relatively rapid changes to the sample composition, the direct sampling with the LMJ-SSP may not appropriately capture them given the length of time required for sample acquisition.

Spatial profiling of microbial colonies is a common process in the discovery of microbial natural products. Heatmaps, which combine the intensity of certain m/z and location information, are usually plotted to visualize the result. *P. tunicata* and *P. rubra* are chosen as they are known to produce tambjamine[38,48] (tambjamine MYP1, $[M + H]^+$ = 354.25; tambjamine YP1, $[M + H]^+$=356.25) and prodiginine[20] compounds (cycloprodigiosin, $[M + H]^+$ = 322.2; prodigiosin, $[M + H]^+$ = 324.2).

As we can see in Figures 2 and 3, the colonies of *P. tunicata* can be well visualized as heatmaps of tambjamines MYP1 and

https://doi.org/10.1021/acsmeasuresciau.4c00035
ACS Meas. Sci. Au 2024, 4, 668−677

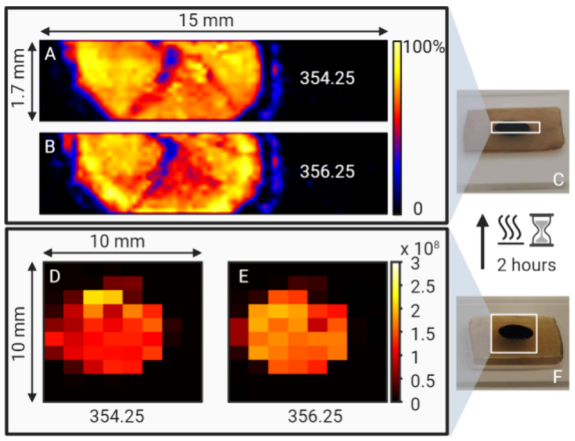

Figure 2. DESI and LMJ-SSP based spatial profiling (A: heatmap of m/z 354.25 from DESI; B: heatmap of m/z 356.25 from DESI; C: colony of *P. tunicata* before sampling by DESI; D: heatmap of m/z 354.25 from LMJ-SSP; E: heatmap of m/z 356.25 from LMJ-SSP; F: colony of *P. tunicata* before sampling by LMJ-SSP).

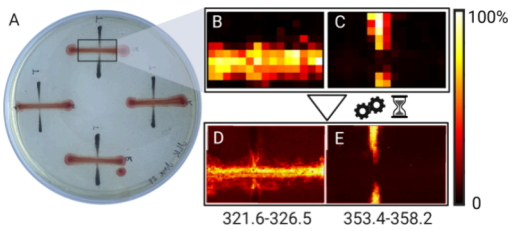

Figure 3. MS imaging for the same interaction area of *P. rubra* and *P. tunicata* using MALDI and LMJ-SSP (A: photo of the agar plate cross streaked with *P. rubra* and *P. tunicata*; B: heatmap of m/z 321.6−326.5 by LMJ-SSP; C: heatmap of m/z 353.4−358.2 by LMJ-SSP; D: heatmap of m/z 321.6−326.5 by MALDI; E: heatmap of m/z 353.4−358.2 by MALDI).

YP1 (Figure 2A,B), whereas the interaction between *P. rubra* and *P. tunicata* (Figure 2D,E) can also be visualized as heatmaps of their natural products. A range of m/z values, instead of a single m/z value, is used to enhance the contrast of the heatmap. Spatial resolution generated by both MALDI and DESI is superior, so we can spot more intricate details of the colonies. Heat maps of tambjamines MYP1 and YP1 are impacted by a slight crack in the dehydrated colony at the center because the DESI signal is vulnerable to surface features (Figure 2A,B). It is also interesting to note that the boundary of *P. tunicata* at the intersection of the two bacterial colonies is surrounded by metabolites from *P. rubra* (Figure 3D). Despite the lower spatial resolution (1 mm), the heatmap from the LMJ-SSP matches well with the results from both MALDI and DESI. No doubt micrometer scale resolution could reveal important information in spatial metabolomics research (for instance: *in situ* host−microbe interactions,[12] cell scale diagnosis[49]) but may not be necessary for all studies.[50] Higher spatial resolution heatmaps from MALDI and DESI tell a similar story but cost extra time and effort.

Highly Robust Hyperspectral Visualization Workflow

Hyperspectral visualization has been demonstrated as a straightforward way to interpret MSI data set as it converts high dimensional molecular features into color-coded images.[38] We previously provided preliminary evidence of hyperspectral visualization as an effective tool in the discovery of microbial natural products, specifically demonstrating that color differences were more straightforward to identify than inspecting individual spectra for changes to metabolite production.[18] To further explore the utilization of hyperspectral visualization-based MSI, MS data sets generated using different ionization techniques are tested with different multivariant analysis methods. Bacteria in different interaction/growth scenarios are also tested.

In the interaction analysis of *P. rubra* and *P. tunicata* (Figure 4B), different multivariate analysis methods are used in the

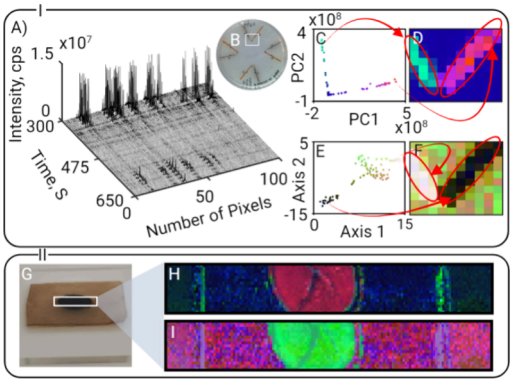

Figure 4. Robustness of hyperspectral visualization based MSI using different algorithms (I) and MS techniques (II) (A: 3D plot of data set acquired by LMJ-SSP; B: photo of sampled area; C: scoring plot by PCA; D: hyperspectral image of microbial interaction based on PCA; E: scoring plot by t-SNE; F: hyperspectral image of microbial interaction based on t-SNE; G: *P. tunicata* colony sampled by DESI; H: hyperspectral image based on PCA; I: hyperspectral image based on t-SNE).

hyperspectral visualization (Figure 4, part I). Spectra (Figure 4A) from each pixel are clustered in a scoring plot by PCA (Figure 4C) and t-SNE (Figure 4E). To make the scoring plot (Figure 4C,E) straightforward, scores of each pixel are converted to RGB values and assembled into colorful maps (Figure 4D,F). It is not difficult to tell the difference between colony and noncolony portions of the sample using hyperspectral images without any background metabolites information (Figure 4D,F). Different species (*P. rubra* and *P. tunicata*) are also visualized with different colors in their hyperspectral images (Figure 4D,F).

To demonstrate that the hyperspectral visualization workflow is not limited to the LMJ-SSP data, data sets generated by DESI were also tested (Figure 4, part II). Similarly, the dimensionality of the data set is reduced first, and an RGB color-coded map is then generated to visualize molecular features of the sampled area (Figure 4G). Both PCA (Figure 4H) and t-SNE (Figure 4I) are used for the data set generated by DESI. As expected, straightforward color maps can be created to visualize the differences between colony and noncolony areas (Figure 4H,I). As the spatial resolution of DESI is high, the crack on the dehydrated colony surface can also be spotted in the hyperspectral images.

PCA and t-SNE are chosen as typical linear and nonlinear multivariant analysis methods in the hyperspectral visualization of *P. rubra* and *P. tunicata*. The shape of colonies can be clearly visualized, and different species are presented with obvious color differences from unsupervised hyperspectral visualization (Figure 4D,F,H,I) Although not surprising,[38,39,51] it is still positive to see that hyperspectral visualization can be used with

https://doi.org/10.1021/acsmeasuresciau.4c00035
ACS Meas. Sci. Au 2024, 4, 668−677

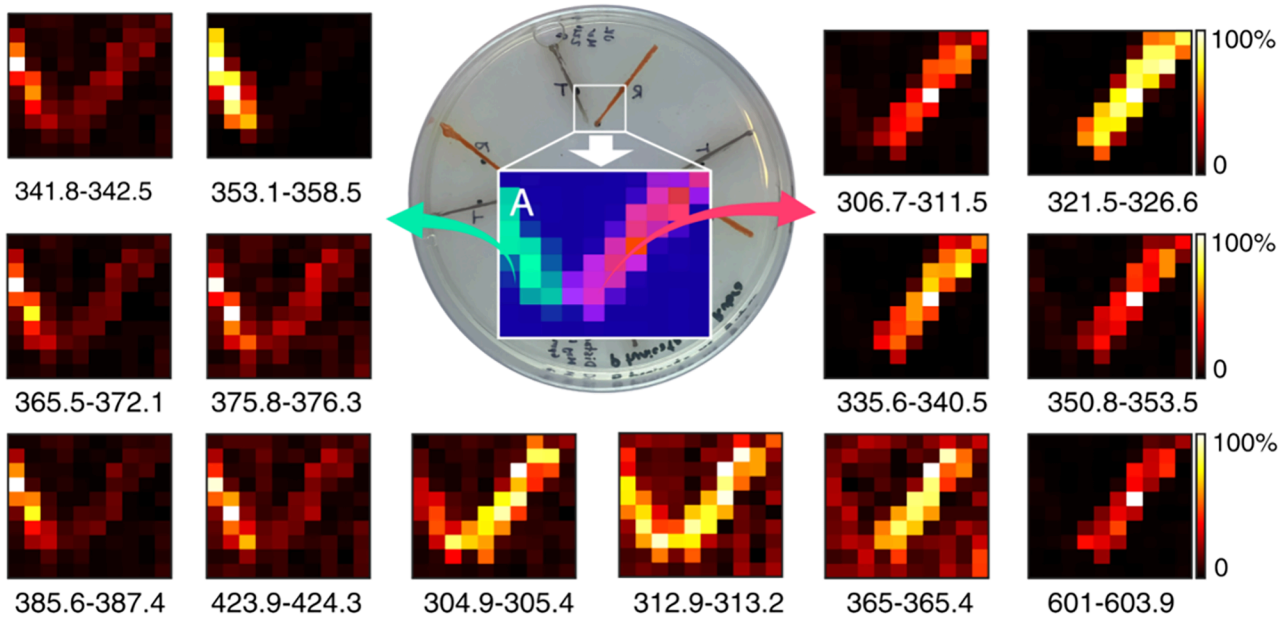

Figure 5. Hyperspectral visualization based MSI for monitoring interactions of *P. rubra* and *P. tunicata* (A: hyperspectral image of sampled area).

linear/nonlinear multivariant analysis of microbial interaction analysis.

PCA and t-SNE have their advantages and disadvantages. PCA has a straightforward loading plot to help us find specific *m/z* corresponding to different colors in the hyperspectral image, whereas t-SNE has better sensitivity.[38,51,52] As robustness and throughput are more important for preliminary scanning of microbial natural products, PCA was chosen for the remaining experiments.

Hyperspectral Visualization in (Static and Temporal) Spatial Metabolome Profiling

PCA based hyperspectral visualization is further explored in static and temporal microbial interaction analysis. In the spatial metabolome analysis of microbial interaction (*P. rubra* and *P. tunicata*), hyperspectral visualization can be used to distinguish molecular profiles from different strains in a straightforward manner with differential coloring (Figure 5A). Molecular features (*m/z* values) corresponding to different species can also be calculated from RGB values in the hyperspectral image.[18] Different *m/z* values can indicate a potential natural product or metabolite. To visualize the distribution of different *m/z*, heatmaps are plotted in Figure 5. In this case, an *m/z* range including accurate *m/z* and its isotopic or isomer *m/z* values is used for heatmap plotting. It is important to understand that the pattern of isotopic peaks is critical to the correct interpretation of *m/z* values. It is not surprising to see heatmaps for multiple molecular features match with each species. As expected, heatmaps of *m/z* 353.1−358.7 and 321.5−326.6 match with tambjamine compounds from *P. tunicata*[18,48] and prodiginine compounds from *P. rubra*.[18,20] Among all heatmaps in Figure 5, *m/z* 304.9−305.4 and 312.9−313.2 can be observed at the tip of the "V" shape (interaction area). These could be either shared primary metabolites from the microorganisms or secondary metabolites of both *P. rubra* and *P. tunicata* (no matches within GNPS). It is interesting to see how PCA based hyperspectral visualization could be used in the temporal analysis of microbial samples (Figure 6). After 24 h of cultivation of *P. rubra* and *P. tunicata*, the emerging red and black color is usually used to confirm their growth. In our

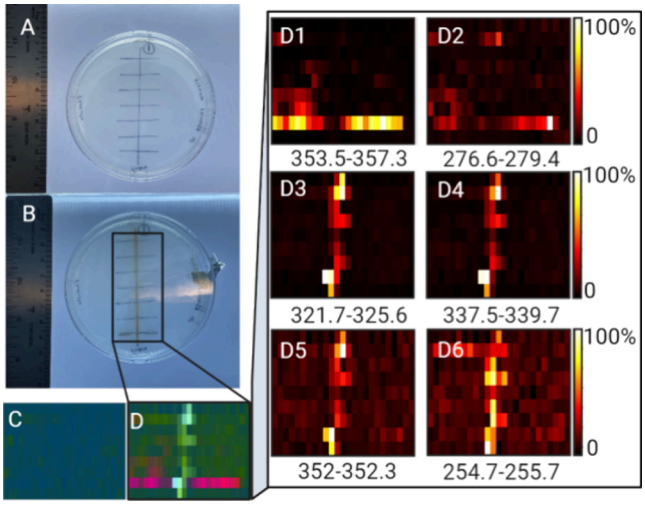

Figure 6. Hyperspectral visualization based MSI on temporal monitoring of *P. rubra* and *P. tunicata* (A: photo of cross streaked *P. rubra* and *P. tunicata* at 0 h after inoculation; B: photo of cross streaked *P. rubra* and *P. tunicata* at 24 h after inoculation; C: hyperspectral image of the cross streaked area at 0 h after inoculation; D: hyperspectral image of the cross streaked area at 24 h after inoculation; D1: heatmap of *m/z* 353.5−357.3; D2: heatmap of *m/z* 276.6−279.4; D3: heatmap of *m/z* 321.7−325.6; D4: heatmap of *m/z* 337.5−339.7; and D5: heatmap of *m/z* 352−352.3, D6: heatmap of *m/z* 254.7−255.7).

research, the data acquired 1 and 24 h after cross streaking on the agar plate are analyzed together by PCA and visualized as described before in Figure 6C,D. It is surprising to find out that the emerging color difference from hyperspectral imaging in Figure 6C,D can visualize the growth of *P. rubra* and *P. tunicata* better than optical images (Figure 6A,B). Molecular features (*m/z* values) related to the growth of *P. rubra* and *P. tunicata* are calculated[18] and plotted as D1−D6 in Figure 6. Tambjamine compounds and prodiginine compounds are found consistent with the growth of *P. tunicata* (Figure 6D1) and *P. rubra* (Figure 6D3), respectively. Heatmaps of several

https://doi.org/10.1021/acsmeasuresciau.4c00035
ACS Meas. Sci. Au 2024, 4, 668−677

other molecular features (Figure 6D2,D4,D5,D6) also match with the growth of *P. rubra* and *P. tunicata*. It could be proposed that they are closely related to microbial growth or interaction.

Follow-up experiments such as larger-scale culturing, extraction, fraction collection, and structure characterization are needed for elucidating the identity and structure of these metabolites, but our direct spatial metabolome scanning approach still provides important indicators for microbial interaction/growth in an extremely rapid and straightforward manner. No complicated sampling alignment is needed as a conductance based automated sampling platform is used.[18,19] Samples can also be preserved for other follow-up experiments if needed. Compared with techniques such as nano-DESI, MALDI, or liquid extraction surface analysis (LESA), significant advantages in throughput and robustness are exhibited for the LMJ-SSP sampling platform when millimeter-level spatial resolution is sufficient.[18,19,27] As our workflow is also integrated with an unsupervised data analysis algorithm, no prior metabolic knowledge about microbial samples is needed.[18,38] Connecting metabolites to specific microorganisms and their interactions is currently a considerable challenge for the natural product community, and the LMJSSP methods described herein will be an important tool for making these connections.[53,54] Our hyperspectral visualization based nondestructive MSI workflow integrates a rapid/robust sample technique, and the straightforward data interpretation method provides an innovative pathway to explore connections in microbial metabolome analysis.

Integrating Spatial Metabolome Profiling with LC–MS

For microbial sample investigation, one of the most important steps is to annotate potentially novel natural products within an untargeted MS data set based on fragmentation data matching.[53] Although various technologies are being rapidly developed in the analysis of microbial samples, LC–MS equipped with untargeted tandem MS fragmentation is still the best option when structure annotation/elucidation is needed. However, as microbial extracts are extremely complicated, it is usually difficult for researchers to decide where to begin when many matches are generated. With few tools or methods available, a typical workflow is to create connections between metabolites and microorganisms with, e.g., spatial metabolome analysis and use the connections to narrow down a target of interest.[53] Our hyperspectral visualization based spatial metabolome profiling workflow is designed to provide straightforward navigation for metabolite annotation in a very rapid and robust way.

Using one of the most popular comparison tools, metabolome data from untargeted LC-MS analysis of *P. tunicata* extract were uploaded to GNPS (Global Natural Products Social Molecular Network)[40] for metabolite annotation. As expected, many molecular networks (30) can be visualized with over 600 nodes (119 library hits). From our earlier result, tambjamine YP1 ([M + H] = *m*/*z* 354.25) is found to be closely related to the growth or development of *P. tunicata*. With such a clue, a small molecular network correlated to tambjamine compounds (Figure 7) could be found among the large amounts of data. From the fragmentation pattern of these four compounds (Figure 7), it can be speculated that *m*/*z* 354.3 is a cyclized molecule (likely tambjamine MYP1),[41,48] whereas *m*/*z* 370.3 and 342.6 are noncyclized tambjamine[55] potentially with different fatty acid

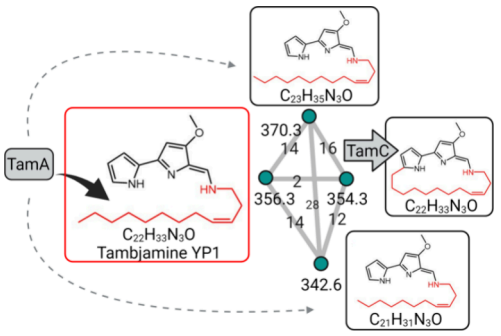

Figure 7. Identification of the molecular network containing tambjamine analogues with different fatty amine tails using the guidance from hyperspectral MSI.

tails. This is the first time that unknown tambjamine analogues with different chain lengths of fatty acids have been identified in *P. tunicata*. The proposed structures of the tambjamine YP1 analogues observed in the molecular network are supported by previous biochemical characterization of biosynthetic enzymes from the tambjamine YP1 pathway. The adenylation enzyme, TamA, is able to select and activate a range of fatty acids of different chain lengths; should these be carried through subsequent steps in the biosynthesis, it would result in the molecular structures we propose here.[21,56,57] Ultimately, the synchronous utility of various fatty acids during the early growth of *P. tunicata* also demonstrated their vital role to microbial growth.[21,57] This observation demonstrates how results from spatial metabolome analysis can be used to advance not only molecule discovery but also our understanding of microbial processes such as biosynthesis of natural products.

CONCLUSIONS

Using the LMJ-SSP with automated sampling, microbial samples grown on agar plates can be rapidly scanned without sample preparation. The performance of the LMJ-SSP is demonstrated to be functionally equivalent to commercialized MS based microbial analysis methods (e.g., MALDI, direct infusion) in natural product discovery research on *Pseudoalteromonas*. Our lab-developed autosampling platform is robust for analyzing typical microbial agar plates, and no complicated spatial alignment is needed for experimental setup. Samples can also be preserved for follow-up and temporal experiments. Little background knowledge about metabolite identity is needed for making connections[53] as hyperspectral visualization is established based on unsupervised data analysis algorithms.[18,38] Therefore, color-coded hyperspectral images[18,38] generated directly from agar plates could provide rapid navigation for typical metabolite annotation.[53]

LMJ-SSP combined with hyperspectral visualization is a rapid and robust workflow for the spatial metabolome profiling of microbial agar plates. The workflow we describe here is not limited to a specific MS technique or data analysis method; indeed, different sampling techniques and data analysis methods could be adopted in the workflow we have presented.

ASSOCIATED CONTENT

Supporting Information

The Supporting Information is available free of charge at https://pubs.acs.org/doi/10.1021/acsmeasuresciau.4c00035.

https://doi.org/10.1021/acsmeasuresciau.4c00035
ACS Meas. Sci. Au 2024, 4, 668–677

Additional experimental details, materials, and methods, including photographs of experimental setup; Figures S1−S3; data to demonstrate schematic of LMJ-SSP; and agar plate being sampled in the current research (PDF)

AUTHOR INFORMATION

Corresponding Author

Richard D. Oleschuk − *Department of Chemistry and Department of Surgery, Queen's University, Kingston, Ontario, Canada K7K 0C2; SCIEX, Concord, Ontario, Canada L4K 4V8;* orcid.org/0000-0003-2783-7532; Email: oleschuk@queensu.ca

Authors

Jian Yu − *Department of Chemistry, Queen's University, Kingston, Ontario, Canada K7K 0C2*

Haidy Metwally − *Department of Chemistry, Queen's University, Kingston, Ontario, Canada K7K 0C2*

Jennifer Kolwich − *Department of Chemistry, Queen's University, Kingston, Ontario, Canada K7K 0C2*

Hailey Tomm − *Department of Chemistry, Queen's University, Kingston, Ontario, Canada K7K 0C2*

Martin Kaufmann − *Department of Surgery, Queen's University, Kingston, Ontario, Canada K7L 2V7*

Rachel Klotz − *Department of Chemistry, Queen's University, Kingston, Ontario, Canada K7K 0C2*

Chang Liu − *SCIEX, Concord, Ontario, Canada L4K 4V8;* orcid.org/0000-0003-0508-4357

J. C. Yves Le Blanc − *SCIEX, Concord, Ontario, Canada L4K 4V8;* orcid.org/0000-0002-3801-3590

Thomas R. Covey − *SCIEX, Concord, Ontario, Canada L4K 4V8*

John Rudan − *Department of Surgery, Queen's University, Kingston, Ontario, Canada K7L 2V7*

Avena C. Ross − *Department of Chemistry, Queen's University, Kingston, Ontario, Canada K7K 0C2;* orcid.org/0000-0002-9845-729X

Complete contact information is available at: https://pubs.acs.org/10.1021/acsmeasuresciau.4c00035

Author Contributions

Professors R.O. and A.C.R. guided all the research work. R.O., A.C.R., J.Y., H.M., and J.K designed the research. R.O., A.C.R., and J.Y. wrote the manuscript. J.Y. and H.M. carried out the MSI and fragmentation experiments. M.K. carried out the DESI experiment. J.Y. performed the data analysis for mass spectrometry data. J.K., H.A.T., and R.K. provided bacteria samples. C.L., Y.L.B., and T.R.C. provided the modified probe for ESI source and advice on LMJ-SSP use. CRediT: **Jian Yu** conceptualization, data curation, formal analysis, investigation, writing - original draft, writing - review & editing; **Haidy Metwally** data curation, formal analysis, investigation, methodology, writing - review & editing; **Jennifer Kolwich** data curation, investigation, validation, writing - review & editing; **Hailey Tomm** data curation, methodology, writing - review & editing; **Martin Kaufmann** data curation, investigation, methodology, visualization, writing - review & editing; **Rachel Klotz** data curation, formal analysis, methodology, writing - review & editing; **Chang Liu** funding acquisition, methodology, resources, supervision, writing - review & editing; **J.C. Yves Le Blanc** funding acquisition, resources, supervision, writing - review & editing; **Thomas R Covey** funding acquisition, resources, supervision, writing - review & editing; **John Rudan** funding acquisition, project administration, supervision; **Avena Clara Ross** conceptualization, data curation, methodology, project administration, supervision, writing - review & editing; **Richard David Oleschuk** conceptualization, funding acquisition, methodology, project administration, resources, supervision, writing - review & editing.

Notes

The authors declare no competing financial interest.

ACKNOWLEDGMENTS

We thank the Natural Sciences and Engineering Research Council (NSERC) for financial support through Discovery (RGPIN RGPIN-2022-03833 to R.O. and 2022-03577 to A.C.R.), New Frontiers in Research Fund (NFRFE-2019-0567 to R.O. and A.C.R.), Strategic Project Grants (STPGP 401252850), Queen's University Wicked Ideas Program, and SCIEX for collaborative, mass spectrometry, and instrumentation support.

REFERENCES

(1) Dunn, W. B.; Broadhurst, D. I.; Atherton, H. J.; Goodacre, R.; Griffin, J. L. Systems Level Studies of Mammalian Metabolomes: The Roles of Mass Spectrometry and Nuclear Magnetic Resonance Spectroscopy. *Chem. Soc. Rev.* **2011**, *40* (1), 387−426.

(2) Metabonomics: Methods and Protocols; Bjerrum, J. T., Ed.; *Methods Mol. Biol.*; Springer New York: New York, NY, 2015; Vol. *1277*. .

(3) Patejko, M.; Jacyna, J.; Markuszewski, M. J. Sample Preparation Procedures Utilized in Microbial Metabolomics: An Overview. *J. Chromatogr. B* **2017**, *1043*, 150−157.

(4) Feider, C. L.; Krieger, A.; DeHoog, R. J.; Eberlin, L. S. Ambient Ionization Mass Spectrometry: Recent Developments and Applications. *Anal. Chem.* **2019**, *91* (7), 4266−4290.

(5) Li, X.; Yin, R.; Hu, H.; Li, Y.; Sun, X.; Dey, S. K.; Laskin, J. An Integrated Microfluidic Probe for Mass Spectrometry Imaging of Biological Samples. *Angew. Chem., Int. Ed.* **2020**, *59* (50), 22388−22391.

(6) Nguyen, S. N.; Sontag, R. L.; Carson, J. P.; Corley, R. A.; Ansong, C.; Laskin, J. Towards High-Resolution Tissue Imaging Using Nanospray Desorption Electrospray Ionization Mass Spectrometry Coupled to Shear Force Microscopy. *J. Am. Soc. Mass Spectrom.* **2018**, *29* (2), 316−322.

(7) Hale, O. J.; Cooper, H. J. Native Mass Spectrometry Imaging of Proteins and Protein Complexes by Nano-DESI. *Anal. Chem.* **2021**, *93* (10), 4619−4627.

(8) Meng, Y.; Song, X.; Zare, R. N. Laser Ablation Electrospray Ionization Achieves 5 Mm Resolution Using a Microlensed Fiber. *Anal. Chem.* **2022**, *94* (28), 10278−10282.

(9) Yin, R.; Burnum-Johnson, K. E.; Sun, X.; Dey, S. K.; Laskin, J. High Spatial Resolution Imaging of Biological Tissues Using Nanospray Desorption Electrospray Ionization Mass Spectrometry. *Nat. Protoc.* **2019**, *14* (12), 3445−3470.

(10) Swales, J. G.; Tucker, J. W.; Strittmatter, N.; Nilsson, A.; Cobice, D.; Clench, M. R.; Mackay, C. L.; Andren, P. E.; Takáts, Z.; Webborn, P. J. H.; Goodwin, R. J. A. Mass Spectrometry Imaging of Cassette-Dosed Drugs for Higher Throughput Pharmacokinetic and Biodistribution Analysis. *Anal. Chem.* **2014**, *86* (16), 8473−8480.

(11) Kompauer, M.; Heiles, S.; Spengler, B. Atmospheric Pressure MALDI Mass Spectrometry Imaging of Tissues and Cells at 1.4-Mm Lateral Resolution. *Nat. Methods* **2017**, *14* (1), 90−96.

(12) Geier, B.; Sogin, E. M.; Michellod, D.; Janda, M.; Kompauer, M.; Spengler, B.; Dubilier, N.; Liebeke, M. Spatial Metabolomics of in Situ Host−Microbe Interactions at the Micrometre Scale. *Nat. Microbiol.* **2020**, *5* (3), 498−510.

(13) Bien, T.; Koerfer, K.; Schwenzfeier, J.; Dreisewerd, K.; Soltwisch, J. Mass Spectrometry Imaging to Explore Molecular Heterogeneity in Cell Culture. *Proc. Natl. Acad. Sci. U. S. A.* **2022**, *119* (29), No. e2114365119.
(14) O'Neill, K. C.; Liapis, E.; Harris, B. T.; Perlin, D. S.; Carter, C. L. Mass Spectrometry Imaging Discriminates Glioblastoma Tumor Cell Subpopulations and Different Microvascular Formations Based on Their Lipid Profiles. *Sci. Rep.* **2022**, *12* (1), 17069.
(15) Wang, M. F.; Joignant, A. N.; Sohn, A. L.; Garrard, K. P.; Muddiman, D. C. Time of Acquisition and High Spatial Resolution Mass Spectrometry Imaging. *J. Mass Spectrom.* **2023**, *58* (3), No. e4911.
(16) Körber, A.; Keelor, J. D.; Claes, B. S. R.; Heeren, R. M. A.; Anthony, I. G. M. Fast Mass Microscopy: Mass Spectrometry Imaging of a Gigapixel Image in 34 minutes. *Anal. Chem.* **2022**, *94* (42), 14652−14658.
(17) Jiang, L.-X.; Yang, M.; Wali, S. N.; Laskin, J. High-Throughput Mass Spectrometry Imaging of Biological Systems: Current Approaches and Future Directions. *TrAC Trends Anal. Chem.* **2023**, *163*, No. 117055.
(18) Yu, J.; Hermann, M.; Smith, R.; Tomm, H.; Metwally, H.; Kolwich, J.; Liu, C.; Le Blanc, J. C. Y.; Covey, T. R.; Ross, A. C.; Oleschuk, R. Hyperspectral Visualization-Based Mass Spectrometry Imaging by LMJ-SSP: A Novel Strategy for Rapid Natural Product Profiling in Bacteria. *Anal. Chem.* **2023**, *95* (3), 2020−2028.
(19) Hermann, M.; Metwally, H.; Yu, J.; Smith, R.; Tomm, H.; Kaufmann, M.; Ren, K. Y. M.; Liu, C.; LeBlanc, Y.; Covey, T. R.; Ross, A. C.; Oleschuk, R. D. 3D Printer Platform and Conductance Feedback Loop for Automated Imaging of Uneven Surfaces by Liquid Microjunction-surface Sampling Probe Mass Spectrometry. *Rapid Commun. Mass Spectrom.* **2023**.
(20) Setiyono, E.; Adhiwibawa, M. A. S.; Indrawati, R.; Prihastyanti, M. N. U.; Shioi, Y.; Brotosudarmo, T. H. P. An Indonesian Marine Bacterium, Pseudoalteromonas Rubra, Produces Antimicrobial Prodiginine Pigments. *ACS Omega* **2020**, *5* (9), 4626−4635.
(21) Marchetti, P. M.; Kelly, V.; Simpson, J. P.; Ward, M.; Campopiano, D. J. The Carbon Chain-Selective Adenylation Enzyme TamA: The Missing Link between Fatty Acid and Pyrrole Natural Product Biosynthesis. *Org. Biomol. Chem.* **2018**, *16* (15), 2735−2740.
(22) Herigstad, B.; Hamilton, M.; Heersink, J. How to Optimize the Drop Plate Method for Enumerating Bacteria. *J. Microbiol. Methods* **2001**, *44* (2), 121−129.
(23) Lertcanawanichakul, M.; Sawangnop, S. A Comparison of Two Methods Used for Measuring the Antagonistic Activity of Bacillus Species. *Walailak J. Sci. Technol.* **2011**, *5* (2), 161−171.
(24) Balouiri, M.; Sadiki, M.; Ibnsouda, S. K. Methods for in Vitro Evaluating Antimicrobial Activity: A Review. *J. Pharm. Anal.* **2016**, *6* (2), 71−79.
(25) Wachs, T.; Henion, J. Electrospray Device for Coupling Microscale Separations and Other Miniaturized Devices with Electrospray Mass Spectrometry. *Anal. Chem.* **2001**, *73* (3), 632−638.
(26) Van Berkel, G. J.; Sanchez, A. D.; Quirke, J. M. E. Thin-Layer Chromatography and Electrospray Mass Spectrometry Coupled Using a Surface Sampling Probe. *Anal. Chem.* **2002**, *74* (24), 6216−6223.
(27) Simon, D.; Oleschuk, R. The Liquid Micro Junction-Surface Sampling Probe (LMJ-SSP); a Versatile Ambient Mass Spectrometry Interface. *Analyst* **2021**, *146* (21), 6365−6378.
(28) Singhal, N.; Kumar, M.; Kanaujia, P. K.; Virdi, J. S. MALDI-TOF Mass Spectrometry: An Emerging Technology for Microbial Identification and Diagnosis. *Front. Microbiol.* **2015**, *6*, 791.
(29) Santos, I. C.; Hildenbrand, Z. L.; Schug, K. A. Applications of MALDI-TOF MS in Environmental Microbiology. *Analyst* **2016**, *141* (10), 2827−2837.
(30) Maier, T.; Klepel, S.; Renner, U.; Kostrzewa, M. Fast and Reliable MALDI-TOF MS−Based Microorganism Identification. *Nat. Methods* **2006**, *3* (4), i−ii.
(31) Hoffmann, T.; Dorrestein, P. C. Homogeneous Matrix Deposition on Dried Agar for MALDI Imaging Mass Spectrometry of Microbial Cultures. *J. Am. Soc. Mass Spectrom.* **2015**, *26* (11), 1959−1962.
(32) McCaughey, C. S.; Trebino, M. A.; Yildiz, F. H.; Sanchez, L. M.Utilizing Imaging Mass Spectrometry to Analyze Microbial Biofilm Chemical Responses to Exogenous Compounds. In *Methods in Enzymology*; Elsevier, 2022; Vol. *665*, pp 281−304. .
(33) Mass Spectrometry Imaging of Small Molecules: Methods and Protocols; Lee, Y.-J., Ed.; *Methods Mol. Biol.*; Springer US: New York, NY, 2022; Vol. *2437*. .
(34) Parrot, D.; Papazian, S.; Foil, D.; Tasdemir, D. Imaging the Unimaginable: Desorption Electrospray Ionization − Imaging Mass Spectrometry (DESI-IMS) in Natural Product Research. *Planta Med.* **2018**, *84* (09/10), 584−593.
(35) Takáts, Z.; Wiseman, J. M.; Cooks, R. G. Ambient Mass Spectrometry Using Desorption Electrospray Ionization (DESI): Instrumentation, Mechanisms and Applications in Forensics, Chemistry, and Biology. *J. Mass Spectrom.* **2005**, *40* (10), 1261−1275.
(36) Venter, A.; Sojka, P. E.; Cooks, R. G. Droplet Dynamics and Ionization Mechanisms in Desorption Electrospray Ionization Mass Spectrometry. *Anal. Chem.* **2006**, *78* (24), 8549−8555.
(37) Angolini, C. F. F.; Vendramini, P. H.; Araújo, F. D. S.; Araújo, W. L.; Augusti, R.; Eberlin, M. N.; de Oliveira, L. G. Direct Protocol for Ambient Mass Spectrometry Imaging on Agar Culture. *Anal. Chem.* **2015**, *87* (13), 6925−6930.
(38) Fonville, J. M.; Carter, C. L.; Pizarro, L.; Steven, R. T.; Palmer, A. D.; Griffiths, R. L.; Lalor, P. F.; Lindon, J. C.; Nicholson, J. K.; Holmes, E.; Bunch, J. Hyperspectral Visualization of Mass Spectrometry Imaging Data. *Anal. Chem.* **2013**, *85* (3), 1415−1423.
(39) Basu, S. S.; Regan, M. S.; Randall, E. C.; Abdelmoula, W. M.; Clark, A. R.; Gimenez-Cassina Lopez, B.; Cornett, D. S.; Haase, A.; Santagata, S.; Agar, N. Y. R. Rapid MALDI Mass Spectrometry Imaging for Surgical Pathology. *Npj Precis. Oncol.* **2019**, *3* (1), 17.
(40) Wang, M.; Carver, J. J.; Phelan, V. V.; Sanchez, L. M.; Garg, N.; Peng, Y.; Nguyen, D. D.; Watrous, J.; Kapono, C. A.; Luzzatto-Knaan, T.; Porto, C.; Bouslimani, A.; Melnik, A. V.; Meehan, M. J.; Liu, W.-T.; Crüsemann, M.; Boudreau, P. D.; Esquenazi, E.; Sandoval-Calderón, M.; Kersten, R. D.; Pace, L. A.; Quinn, R. A.; Duncan, K. R.; Hsu, C.-C.; Floros, D. J.; Gavilan, R. G.; Kleigrewe, K.; Northen, T.; Dutton, R. J.; Parrot, D.; Carlson, E. E.; Aigle, B.; Michelsen, C. F.; Jelsbak, L.; Sohlenkamp, C.; Pevzner, P.; Edlund, A.; McLean, J.; Piel, J.; Murphy, B. T.; Gerwick, L.; Liaw, C.-C.; Yang, Y.-L.; Humpf, H.-U.; Maansson, M.; Keyzers, R. A.; Sims, A. C.; Johnson, A. R.; Sidebottom, A. M.; Sedio, B. E.; Klitgaard, A.; Larson, C. B.; Boya P, C. A.; Torres-Mendoza, D.; Gonzalez, D. J.; Silva, D. B.; Marques, L. M.; Demarque, D. P.; Pociute, E.; O'Neill, E. C.; Briand, E.; Helfrich, E. J. N.; Granatosky, E. A.; Glukhov, E.; Ryffel, F.; Houson, H.; Mohimani, H.; Kharbush, J. J.; Zeng, Y.; Vorholt, J. A.; Kurita, K. L.; Charusanti, P.; McPhail, K. L.; Nielsen, K. F.; Vuong, L.; Elfeki, M.; Traxler, M. F.; Engene, N.; Koyama, N.; Vining, O. B.; Baric, R.; Silva, R. R.; Mascuch, S. J.; Tomasi, S.; Jenkins, S.; Macherla, V.; Hoffman, T.; Agarwal, V.; Williams, P. G.; Dai, J.; Neupane, R.; Gurr, J.; Rodríguez, A. M. C.; Lamsa, A.; Zhang, C.; Dorrestein, K.; Duggan, B. M.; Almaliti, J.; Allard, P.-M.; Phapale, P.; Nothias, L.-F.; Alexandrov, T.; Litaudon, M.; Wolfender, J.-L.; Kyle, J. E.; Metz, T. O.; Peryea, T.; Nguyen, D.-T.; VanLeer, D.; Shinn, P.; Jadhav, A.; Müller, R.; Waters, K. M.; Shi, W.; Liu, X.; Zhang, L.; Knight, R.; Jensen, P. R.; Palsson, B. Ø.; Pogliano, K.; Linington, R. G.; Gutiérrez, M.; Lopes, N. P.; Gerwick, W. H.; Moore, B. S.; Dorrestein, P. C.; Bandeira, N. Sharing and Community Curation of Mass Spectrometry Data with Global Natural Products Social Molecular Networking. *Nat. Biotechnol.* **2016**, *34* (8), 828−837.
(41) Picott, K. J.*Biosynthesis of Prodiginne and Tambjamine Natural Products in Psudoalteromonas Sp.*; Queen's University, 2018, 1−151.
(42) Jens, J. N.; Breiner, D. J.; Phelan, V. V. Spray-Based Application of Matrix to Agar-Based Microbial Samples for Reproducible Sample Adherence in MALDI MSI. *J. Am. Soc. Mass Spectrom.* **2022**, *33* (4), 731−734.

(43) Ho, Y.-N.; Shu, L.-J.; Yang, Y.-L. Imaging Mass Spectrometry for Metabolites: Technical Progress, Multimodal Imaging, and Biological Interactions. *WIREs Syst. Biol. Med.* **2017**, *9* (5), No. e1387.
(44) Li, B.; Comi, T. J.; Si, T.; Dunham, S. J. B.; Sweedler, J. V. A One-Step Matrix Application Method for MALDI Mass Spectrometry Imaging of Bacterial Colony Biofilms. *J. Mass Spectrom. JMS* **2016**, *51* (11), 1030−1035.
(45) Yang, Y.-L. Translating Metabolic Exchange with Imaging Mass Spectrometry. *Nat. Chem. Biol.* **2009**, *5* (12), 885.
(46) Takáts, Z.; Wiseman, J. M.; Gologan, B.; Cooks, R. G. Mass Spectrometry Sampling Under Ambient Conditions with Desorption Electrospray Ionization. *Science* **2004**, *306* (5695), 471−473.
(47) Watrous, J.; Hendricks, N.; Meehan, M.; Dorrestein, P. C. Capturing Bacterial Metabolic Exchange Using Thin Film Desorption Electrospray Ionization-Imaging Mass Spectrometry. *Anal. Chem.* **2010**, *82* (5), 1598−1600.
(48) Picott, K. J.; Deichert, J. A.; deKemp, E. M.; Schatte, G.; Sauriol, F.; Ross, A. C. Isolation and Characterization of Tambjamine MYP1, a Macrocyclic Tambjamine Analogue from Marine Bacterium *Pseudoalteromonas Citrea*. *MedChemComm* **2019**, *10* (3), 478−483.
(49) Luo, L.; Ma, W.; Liang, K.; Wang, Y.; Su, J.; Liu, R.; Liu, T.; Shyh-Chang, N. Spatial Metabolomics Reveals Skeletal Myofiber Subtypes. *Sci. Adv.* **2023**, *9* (5), No. eadd0455.
(50) Watrous, J.; Roach, P.; Heath, B.; Alexandrov, T.; Laskin, J.; Dorrestein, P. C. Metabolic Profiling Directly from the Petri Dish Using Nanospray Desorption Electrospray Ionization Imaging Mass Spectrometry. *Anal. Chem.* **2013**, *85* (21), 10385−10391.
(51) Abdelmoula, W. M.; Balluff, B.; Englert, S.; Dijkstra, J.; Reinders, M. J. T.; Walch, A.; McDonnell, L. A.; Lelieveldt, B. P. F. Data-Driven Identification of Prognostic Tumor Subpopulations Using Spatially Mapped t-SNE of Mass Spectrometry Imaging Data. *Proc. Natl. Acad. Sci. U. S. A.* **2016**, *113* (43), 12244−12249.
(52) Maaten, L. V. D.; Hinton, G. E.*Visualizing Data using t-SNE*. undefined. /paper/Visualizing-Data-using-t-SNE-Maaten-Hinton/1c46943103bd7b7a2c7be86859995a4144d1938b (accessed 2021−03−01).
(53) Bauermeister, A.; Mannochio-Russo, H.; Costa-Lotufo, L. V.; Jarmusch, A. K.; Dorrestein, P. C. Mass Spectrometry-Based Metabolomics in Microbiome Investigations. *Nat. Rev. Microbiol.* **2022**, *20* (3), 143−160.
(54) Bouslimani, A.; Porto, C.; Rath, C. M.; Wang, M.; Guo, Y.; Gonzalez, A.; Berg-Lyon, D.; Ackermann, G.; Moeller Christensen, G. J.; Nakatsuji, T.; Zhang, L.; Borkowski, A. W.; Meehan, M. J.; Dorrestein, K.; Gallo, R. L.; Bandeira, N.; Knight, R.; Alexandrov, T.; Dorrestein, P. C. Molecular Cartography of the Human Skin Surface in 3D. *Proc. Natl. Acad. Sci. U. S. A.* **2015**, *112* (17), E2120−E2129.
(55) Burke, C.; Thomas, T.; Egan, S.; Kjelleberg, S. The Use of Functional Genomics for the Identification of a Gene Cluster Encoding for the Biosynthesis of an Antifungal Tambjamine in the Marine Bacterium Pseudoalteromonas Tunicata. *Environ. Microbiol.* **2007**, *9* (3), 814−818.
(56) Marchetti, P. M.; Richardson, S. M.; Kariem, N. M.; Campopiano, D. J. Synthesis of *N* -Acyl Amide Natural Products Using a Versatile Adenylating Biocatalyst. *MedChemComm* **2019**, *10* (7), 1192−1196.
(57) Cronan, J. E.; Thomas, J.Chapter 17 Bacterial Fatty Acid Synthesis and Its Relationships with Polyketide Synthetic Pathways. In *Methods in Enzymology*; Elsevier, 2009; Vol. *459*, pp 395−433. .

https://doi.org/10.1021/acsmeasuresciau.4c00035
ACS Meas. Sci. Au 2024, 4, 668−677